Spectroscopic Study of Ser92 Mutants of Human Myoglobin: Hydrogen Bonding Effect of Ser92 to Proximal His93 on Structure and Property of Myoglobin†

Yoshitsugu Shiro,*,‡ Tetsutaro Iizuka,‡ Koji Marubayashi,§ Takashi Ogura,|| Teizo Kitagawa,|| Sriram Balasubramanian,⊥ and Steven G. Boxer⊥

The Institute of Physical and Chemical Research (RIKEN), Wako, Saitama 351-01, Japan, Faculty of Science, Gakusyuin University, Mejiro, Toshima-ku, Tokyo 170, Japan, The Institute for Molecular Science, Okazaki National Research Institutes, Nyodaiji, Okazaki 444, Japan, and Department of Chemistry, Stanford University, Stanford, California 94305-5080

Received June 8, 1994; Revised Manuscript Received September 1, 1994⊗

ABSTRACT: Neutron diffraction studies have demonstrated that the hydroxyl group oxygen of Ser92(F7) is hydrogen bonded to the proximal His93(48) $N^{\epsilon}H$ proton in myoglobin (Mb) [Cheng, X., & Shoenborn, B. P. (1991) *J. Mol. Biol. 220*, 381−399]. In order to examine the importance of this hydrogen bond, Ser92 was replaced with Ala and Asp in human Mb. By comparing the optical, ^{1}H-NMR, resonance Raman, and IR spectra of Mb(S92A) in several spin and oxidation states with those of wild-type Mb, it was found that the mutation causes a structural change on the heme proximal side but not on the distal side. Comparison of the NMR spectra of the cyanomet form of Mb(S92A) and Mb(WT) suggests that the imidazole plane of His93 rotates somewhat around the Fe−N^{δ}(His93) bond upon loss of the hydrogen bond between His93 and Ser92. The 2D ^{1}H-NMR measurements of the CO complexes show that mutation of Ser92 to Ala changes the relative position of the His97 imidazole group to the heme plane, but the change is not so drastic as reported in the crystal data of Ser92 mutant of pig Mb [Smerdon et al. (1993) *Biochemistry 32*, 5132−5138]. On the other hand, ligand (CO, O_2) binding is only slightly affected by this mutation. From these results, we conclude that the Ser92−His93 hydrogen bond maintains the protein structure of the proximal heme pocket, but it does not strongly affect the electronic structure of the heme as well as of the His93 imidazole ring. Although Mb(S92D) proved to be very unstable; limited comparisons were possible, suggesting surprisingly that Mb(S92D) is very similar to Mb(S92A).

In hemoproteins, iron reactivity is electronically and/or sterically controlled through the iron axial ligand. The original Perutz model for hemoglobin cooperativity emphasized a strained or stretched iron−histidine (proximal His) bond, where the change of the Fe−imidazole bond modulates the quaternary structure and consequently the oxygen affinity (Perutz, 1970). It is also recognized that the formation of a hydrogen bond between the proximal His imidazole $N^{\epsilon}H$ and a protein acceptor residue can modulate the Fe−imidazole bond and, consequently, the iron reactivity. For example, significant anionic character of the proximal His174 in cytochrome *c* peroxidase (CCP) resulting from a strong hydrogen bond between its $N^{\epsilon}H$ and the carboxylate of Asp235 (Poulos et al., 1980) is the primary cause of the unusual and biologically significant properties of CCP, such as its extremely low redox potential and stabilization of higher oxidation states of the heme iron.

Recently, X-ray crystallographic studies of sperm whale and horse Mbs (Oldfield et al., 1992; Evans & Brayer, 1990) suggested that the proximal His, His93(F8), interacts with a hydroxyl oxygen of Ser92(F7) via a hydrogen bond. In addition, a neutron diffraction study by Cheng and Schoenborn (1991) determined its steric geometry; the O(Ser92) to H(His93) hydrogen bond distance is 2.51 Å, the O(Ser92) to N^{ϵ}(His93) distance is 3.16 Å, and the O−H−N bond angle is 123°. The Ser92−His93 hydrogen bond had never been identified until these crystallographic studies were reported, so that the His93 imidazole NH is now recognized to interact through the hydrogen bonds with the Ser92 hydroxy group and the main-chain carbonyl of Leu89(F4). Since Ser92 is highly conserved in all mammalian Mbs,[1] the hydrogen bond of His93 imidazole with the Ser92 hydroxy group is possibly significant in regulating the structure and/or function of Mb.

To test the effect of the His93−Ser92 hydrogen bond, Smerdon et al. (1993) recently prepared site-directed mutants of Ser92 in pig Mb, where the Ser92 residue was replaced with Ala, Val, and Leu, and studied the ligand binding kinetics of these mutants and the X-ray crystal structure of the Leu92 mutant. In this study, they showed that the hydrogen bonding network at the heme proximal side has been disrupted upon replacement of Ser92 with the aliphatic residues, leading to a more exposed proximal pocket which allows the heme to easily dissociate from the protein.

Independently of the work by Smerdon and his co-workers, we also prepared the Ser92 mutants of human Mb, where Ser92 was replaced with Ala and Asp, and in this paper we report their structural characterization in the solution state using some spectroscopic methods. Sometimes the solution structure of the protein is subtly different from the crystal structure. In addition, the spectroscopic methods such as NMR and resonance Raman spectroscopies are much more

† This work was supported by the Biodesign Research Program from RIKEN, by Special Coordination Funds of the Science and Technology Agency of the Japanese Government, and by a grant from the National Institutes of Health to S.G.B.

* To whom correspondence should be addressed.
‡ The Institute of Physical and Chemical Research.
§ Gakusyuin University.
|| Okazaki National Research Institutes.
⊥ Stanford University.

⊗ Abstract published in *Advance ACS Abstracts,* November 15, 1994.

[1] The data of Mb primary structure from Protein Identification Resource was aligned by using the program by Higgins and Sharp (1988).

0006-2960/94/0433-14986$04.50/0

sensitive to subtle changes in the local structure of the protein and in the electronic state of the heme−ligands moiety than the crystallographic method. For example, the X-ray crystallographic study of Mb(S92L) showed no structural change on the Fe−imidazole(His93) bond upon the mutation from Ser92 to Leu, although they had expected rotation of the imidazole group around the Fe−N bond by reference to the heme proximal structure in leghemoglobin. In contrast, we could reveal the change in the structure and the electronic state of the Fe−imidazole(His93) moiety (see Discussion). Therefore, our spectroscopic data are complementary to the crystallographic data and provide information that is based on the detailed discussion about the effect of the Ser92−His93 hydrogen bond on the structure and function of Mb.

MATERIALS AND METHODS

Mutagenesis and Protein Purification of Human Mb. Mutagenesis of human Mb was carried out using the PCR method (Balasubramanian et al., 1993). The expression system produces a fusion protein, which upon reconstitution with heme and tryptic digession yields the desired mutant protein by methods that have been described earlier (Varadarajan et al., 1989; Lambright et al., 1989). The buffer solution employed for spectral measurements is 0.1 M potassium phosphate buffer, pH 6.8.

Spectral Measurements. Electronic absorption spectra were recorded at room temperature on a Varian 2300 spectrophotometer. Extinction coefficients were calculated on the basis of the protein concentration determined by the pyridine−hemochrome method.

NMR experiments were conducted at 25 °C and either 500 MHz (GE GN500) or 600 MHz (Bruker AMX600). For detection of H-D exchangeable proton signals, the sample was prepared in the mixed buffer of 90% H_2O and 10% D_2O, and the water signal was suppressed by either a decoupler pulse prior to the observe pulse or the jump-and-return pulse method. Signal assignment was done according to the methods reported previously (Dalvit & Wright, 1987; Varadarajan et al., 1989).

Resonance Raman scattering was excited at 441.6 nm with a He/Cd laser (Kinmon Electronics, CDR80SG) and detected by a JEOL-400D Raman spectrometer equipped with a cooled HTV-943-02 photomultiplier. The frequencies of the Raman spectrometer were calibrated with indene or tetrachloromethane.

Kinetic Measurements of O_2 and CO Binding. The association and the dissociation rate constants of O_2 and the association constant of CO were obtained by a conventional flash photolysis apparatus (UNISOKU, Osaka) under pseudo-first order conditions ([Mb] ≪ [L]). The measurements were carried out under various ligand concentrations, which were controlled by using a gas mixer (ESTEC Model SGD-XC-0.5L). The first-order rate constants, k_{obs}, calculated from the kinetic trace were plotted against the ligand concentration employed, yielding the on-rate constant (k_{on}) and the off-rate constant (k_{off}) from the slope and the intercept in this plot, respectively. The dissociation rate constant of CO was measured by the NO−CO replacement method on a stopped-flow apparatus (UNISOKU, Osaka). Details of the kinetic measurements are reported elsewhere (Sato et al., 1992).

RESULTS

Two mutants of human Mb, Mb(S92A) and Mb(S92D), were prepared by recombinant DNA methods. Mb(S92A) was expressed at high levels in *Escherichia coli* as a fusion protein which, after reconstitution with heme, could be digested with trypsin to give the final protein in good yield. On the other hand, Mb(S92D) was expressed in a very small amount and, following reconstitution with heme, is very unstable to tryptic digestion so that we could not obtain sufficient protein for further study. Therefore, we reconstituted the fusion protein of Mb(S92D) with heme and purified this fusion protein. This strategy is useful for electronic absorption and ^{1}H-NMR spectroscopy, as it has been shown that the hyperfine-shifted peaks in the metCN complex are identical for the WT Mb fusion protein and the pure Mb(WT) protein.[2] We denote the fusion protein as Mb′(S92D) in this paper.

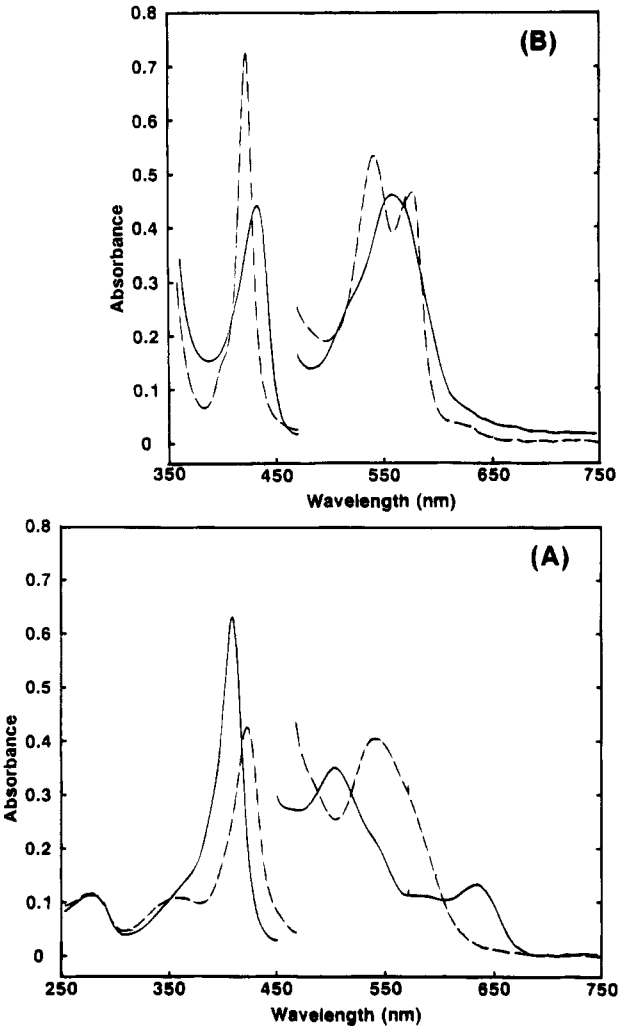

FIGURE 1: Optical absorption spectra of Mb(S92A) in the ferric (A) and in the ferrous (B) states at room temperature and pH 6.8. (A, solid line) aquomet, (A, broken line) cyanomet, (B, solid line) deoxy, and (B, broken line) CO forms of Mb(S92A). To avoid congestion, the spectrum of the oxy form is omitted.

Visible Absorption Spectra in the Ferric and Ferrous States. Figure 1 shows visible absorption spectra of Mb(S92A) in various oxidation and spin states of the heme iron. The wavelength and extinction coefficients at the absorption maxima in the spectra of Mb(S92A) are compiled in Table 1 and are compared with those of Mb(WT). Inspection of Figure 1 and Table 1 shows that the visible spectral properties of Mb(S92A) are essentially the same as those of Mb(WT). This was also the case for Mb′(S92D), indicating that the

[2] D. G. Lambright and S. G. Boxer, unpublished results.

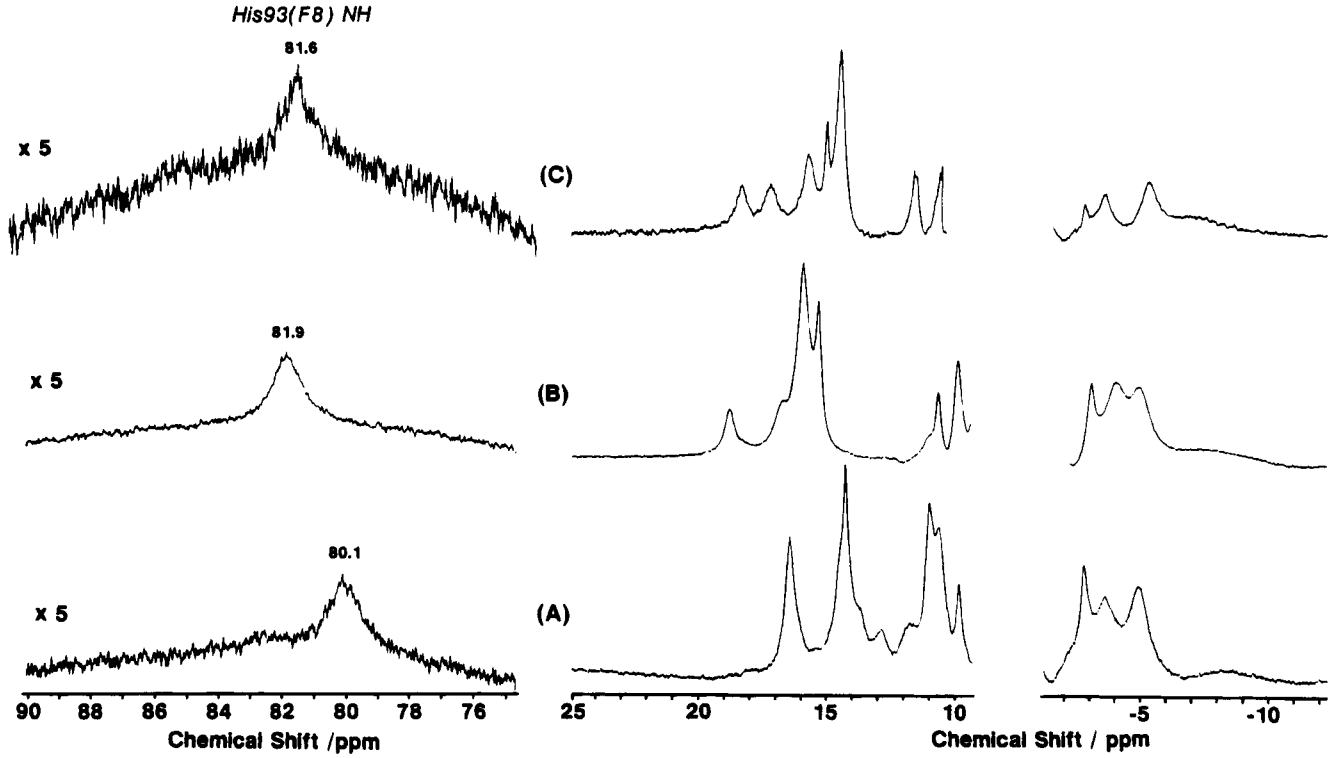

FIGURE 2: ^{1}H-NMR spectra of (A) Mb(WT), (B) Mb(S92A), and (C) Mb′(S92D) in the deoxy form. The spectra were measured in 90% H_2O at 25 °C and pH 6.8. The signals around 80 ppm were not detected in 100% D_2O buffer solution. The sample concentration is about 2 mM for Mb(WT) and Mb(S92A), while less than 1 mM for Mb′(S92D).

Table 1: Wavelength (Extinction Coefficients) of Absorption Maxima in Optical Absorption Spectra of Some Derivatives for Mb(Wild Type) and Mb(Ser92Ala)

	Mb(S92A)			Mb(WT)		
	Soret	visible		Soret	visible	
aquomet	409 (185)	504 (10.1)	633 (3.8)	409 (172)	504 (9.4)	633 (3.5)
CN^-	423 (125)	541 (11.9)		423 (115)	543 (11.5)	
deoxy	433 (129)	558 (13.5)		434 (122)	557 (13.2)	
oxy	418 (128)	543 (13.6)	581 (14.6)	418 (120)	543 (13.0)	581 (13.3)
CO	423 (212)	541 (15.6)	576 (13.7)	422 (199)	540 (15.4)	577 (13.3)

structure in the vicinity of the heme is not drastically altered upon replacing Ser92 with Ala or Asp. Because the structural changes caused by the Ser92 mutation, if any, appear to be subtle, they were studied further by more sensitive spectroscopic methods such as NMR and resonance Raman spectroscopies.

^{1}H-NMR and Resonance Raman Spectra of the Deoxy Form. We measured ^{1}H-NMR spectra of Mb(WT), Mb(S92A), and Mb′(S92D) in the ferrous high spin (deoxy) state. As shown in Figure 2, the hyperfine-shifted proton signals at 10−20 and 0 to −10 ppm, which come from the protons of the heme and nearby protein residues, exhibit different features among the proteins. In addition, a signal with the intensity of one proton was observed at 80.1, 81.9, and 81.6 ppm for Mb(WT), Mb(S92A), and Mb′(S92D), respectively. These signals were not detected in D_2O solution and are assigned to the exchangeable $N^\epsilon H$ proton of His93 (La Mar et al., 1977). These results suggest that the mutation of Ser92 to Ala and Asp does cause a structural change around the proximal His93, but the structural

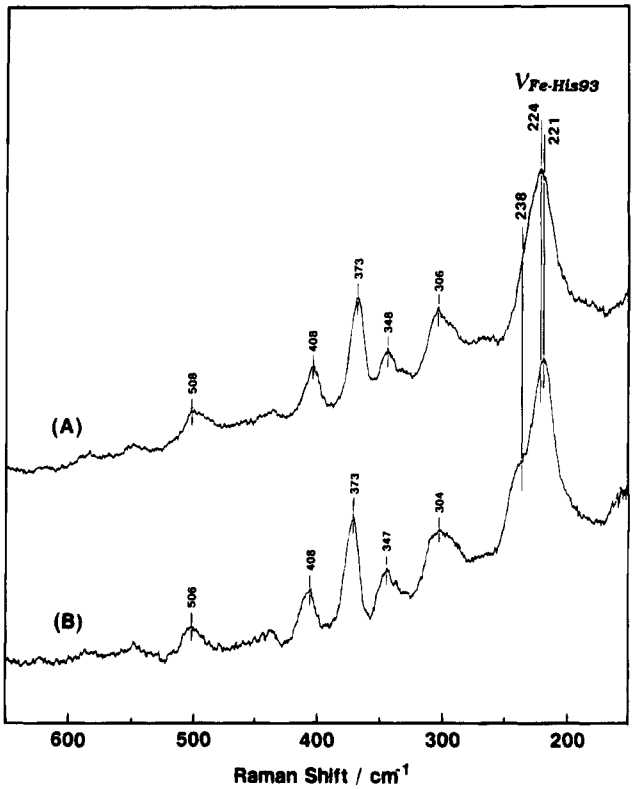

FIGURE 3: Resonance Raman spectra of the deoxy form of (A) Mb(S92A) and (B) Mb(WT) excited by He/Cd laser (441.6 nm). The spectra were measured at room temperature and pH 6.8. The sample concentrations were 40 μM.

difference between Mb(S92A) and Mb′(S92D) appears to be small.

In order to gain further insight into the structure at the heme proximal side, especially the Fe−N^δ(His93) bond character, we measured the resonance Raman spectra of

Table 2: Bimolecular Association and Dissociation Rate Constants of CO and O_2 for Mb(Ser92Ala) and Mb(Wild Type) at 25 °C and pH 7.0

	CO		O_2	
	k_{on} (M^{-1} s^{-1})	k_{off} (s^{-1})	k_{on} (M^{-1} s^{-1})	k_{off} (s^{-1})
Mb(S92A)	1.34×10^6	0.01	2.2×10^7	15
Mb(WT)	1.02×10^6	0.02	2.0×10^7	14

Mb(WT) and Mb(S92A) in the deoxy form. Figure 3 shows the low-frequency region of the Raman spectra measured with a 0.25-cm^{-1} resolution. The spectral features of Mb(S92A) and Mb(WT) are very similar except for the stretching mode of Fe−N^{δ}(His93), which was observed at 221 and 224 cm^{-1} for Mb(WT) and Mb(S92A), respectively. The shoulder on the peak at 238 cm^{-1} in the spectrum of Mb(WT) is not resolved by overlapping with Fe−N^{δ}(His93) stretching peak in that of Mb(S92A). Thus, the 3-cm^{-1} shift of the Fe−N^{δ}(His93) stretch is significant, suggesting that the Fe−N^{δ}(His93) bond is strengthened upon substituting Ser92 with Ala.

CO and O_2 Binding Kinetics. To investigate the change in the properties of Mb upon the mutation of Ser92, we examined the CO and O_2 binding kinetics and obtained the association and the dissociation rate constants for both ligands in the bimolecular reaction. As seen in Table 2, the rate constants were slightly different between these two proteins; the association rate constant is slightly increased upon substitution of Ser92 with Ala, while the dissociation rate constant is essentially unchanged. The kinetic results for human wild-type and S92A Mbs are similar to those reported for pig Mb and its mutants by Smerdon et al. (1993).

^{1}H-NMR Spectra of the CO Form. To characterize the protein structure of Mb(S92A) in the ferrous CO form, we examined its 2-D ^{1}H-NMR (NOESY, COSY, and double quantum) spectra and compared the proton signal positions of the heme and the amino acid residues with those of Mb(WT)CO (Table 3). The heme methyl and vinyl proton signals were not so drastically altered in their positions upon replacement of Ser92 with Ala. The position order of the methyl signals (3-, 1-, 8-, and 5-CH_3 from downfield) is the same between Mb(S92A) and Mb(WT), showing that the heme orientation is normalized in Mb(S92A). On the other hand, the resonance position of the β- and δ-*meso* protons changed more than the other heme proton signals, resulting in the change of the order for the *meso* signal position [γ, δ, α, and β from low to high field in Mb(S92A) compared to γ, α, δ, and β in Mb(WT), see Figure 4A].

The γ-*meso* proton signal of Mb(S92A)CO gives cross peaks with His97(FG3) $C^{\epsilon}H$ signal at 8.20 ppm and His64(E7) $C^{\epsilon}H$ signal at 7.42 ppm in the NOESY spectrum (Figure 4A). Then, their $C^{\delta}H$ signals were easily assigned at 2.76 and 4.98 ppm for His97 and His64, respectively, in the double quantum spectrum (Figure 4B).

The change in the signal positions of the His64 protons in Mb(S92A) is not more than 0.05 ppm relative to Mb(WT). This is also the case for the signals of other distal residues such as Val68(E11), Phe43(CD1), and Phe46(CD4), indicating that the distal side of the heme is unperturbed by change at Ser92. In contrast, there is a substantial change of the His97(FG3) signal position, $\Delta = 0.16$ for $C^{\epsilon}H$ signal and $\Delta = -0.20$ for $C^{\delta}H$ signal. This residue is located close to the heme on the proximal side, so the change in its NMR shifts is indicative of the structural change on the heme proximal side upon changing Ser92 to Ala.

Table 3: Chemical Shifts for Selected Protons Close to the Heme Group in the CO Derivatives of Mb(S92A) and Mb(WT)

		Mb(S92A)CO	Mb(WT)CO	Δ
1-CH3		3.72	3.63	0.09
1-CH3		3.81	3.79	0.02
1-CH3		2.63	2.53	0.10
1-CH3		3.60	3.59	0.01
2-vinyl	H^{α}	8.43	8.43	0
	$H^{\beta}t$	5.7	5.73	0
	$H^{\beta}c$	5.7	5.69	0
4-vinyl	H^{α}	8.66	8.62	0.04
	$H^{\beta}t$	6.68	6.61	0.07
	$H^{\beta}c$	6.32	6.29	0.03
meso	α	9.91	9.95	−0.04
	β	9.51	9.40	0.11
	γ	10.16	10.19	−0.03
	δ	9.97	9.91	0.06
Leu29(B10)	$C^{\delta}H3$	−0.67	−0.71	0.06
	$C^{\delta}H3$	−0.22	−0.29	0.07
Phe33(B14)	$C^{\delta}H$	7.06	7.01	0.05
	$C^{\epsilon}H$	6.53	6.45	0.08
	$C^{\zeta}H$	5.32	5.22	0.10
Phe43(CD1)	$C^{\delta}H$	7.32	7.32	0
	$C^{\epsilon}H$	6.12	6.13	−0.01
	$C^{\zeta}H$	4.82	4.81	0.01
His64(E7)	$C^{\delta}H$	4.98	5.00	−0.02
	$C^{\epsilon}H$	7.42	7.47	−0.05
Val68(E11)	$C^{\gamma}H3$	−2.31	−2.31	0
	$C^{\gamma}H3$	−0.52	−0.59	0.07
	$C^{\alpha}H$	3.30	3.24	0.06
His93(F8)	$C^{\delta}H$	1.16	1.13	0.03
	$C^{\epsilon}H$	1.73	1.67	0.06
His97(FG3)	$C^{\delta}H$	2.76	2.96	−0.20
	$C^{\epsilon}H$	8.20	8.04	0.16

^{1}H-NMR Spectra of the Cyanide Form. The hyperfine-shifted ^{1}H-NMR spectra of the cyanide (CN^-) complex of ferric Mb(WT), Mb(S92A), and Mb′(S92D) are shown in Figure 5. Since the heme orientation is normal for these proteins, as was suggested above, we can assign the heme methyl group signals of Mb(S92A)$^+CN^-$ and Mb′(S92D)$^+CN^-$ by analogy with the spectral pattern of Mb(WT)$^+CN^-$ (Lambright et al., 1989) as shown in Table 4. These heme methyl group signals shift upfield by 2.7−1.7 ppm upon the Ser92 mutation but are located in exactly the same position for Mb(S92A) and Mb′(S92D).

Comparison of the spectra measured in H_2O and D_2O facilitates assignment of the nonlabile and labile proton signals (Varadarajan et al., 1989). We observe an H-D exchangeable proton signal at 22.7 or 22.3 ppm for Mb(S92A) or Mb′(S92D), respectively. Upon raising the pH from 6.8 to 8.0, this signal was decreased in intensity, with concomitant appearance of a new exchangeable peak at 24 ppm as a shoulder of the 5-methyl group signal (data not shown). On the basis of the pH-dependent behavior of these H-D exchangeable peaks, we could assign the signal at 22 ppm to the proximal His93(F8) $N^{\epsilon}H$ and that at 24 ppm to the distal His64(E7) $N^{\epsilon}H$. The mutation of Ser92 to Ala induced a downfield shift for the proximal His $N^{\epsilon}H$ by 1.2 ppm but does not affect the distal His64 $N^{\epsilon}H$.

DISCUSSION

Ala92(F7) Mutant of Myoglobin. In the Ala92(F7) mutant of human Mb, where the Ser residue at the 92(F7) position is replaced with Ala, the hydrogen bonding interaction between the Ser92(F7) hydroxyl group and the His93(F8) $N^{\epsilon}H$ is absent. Therefore, the differences in the NMR and resonance Raman spectra between Mb(S92A) and Mb(WT)

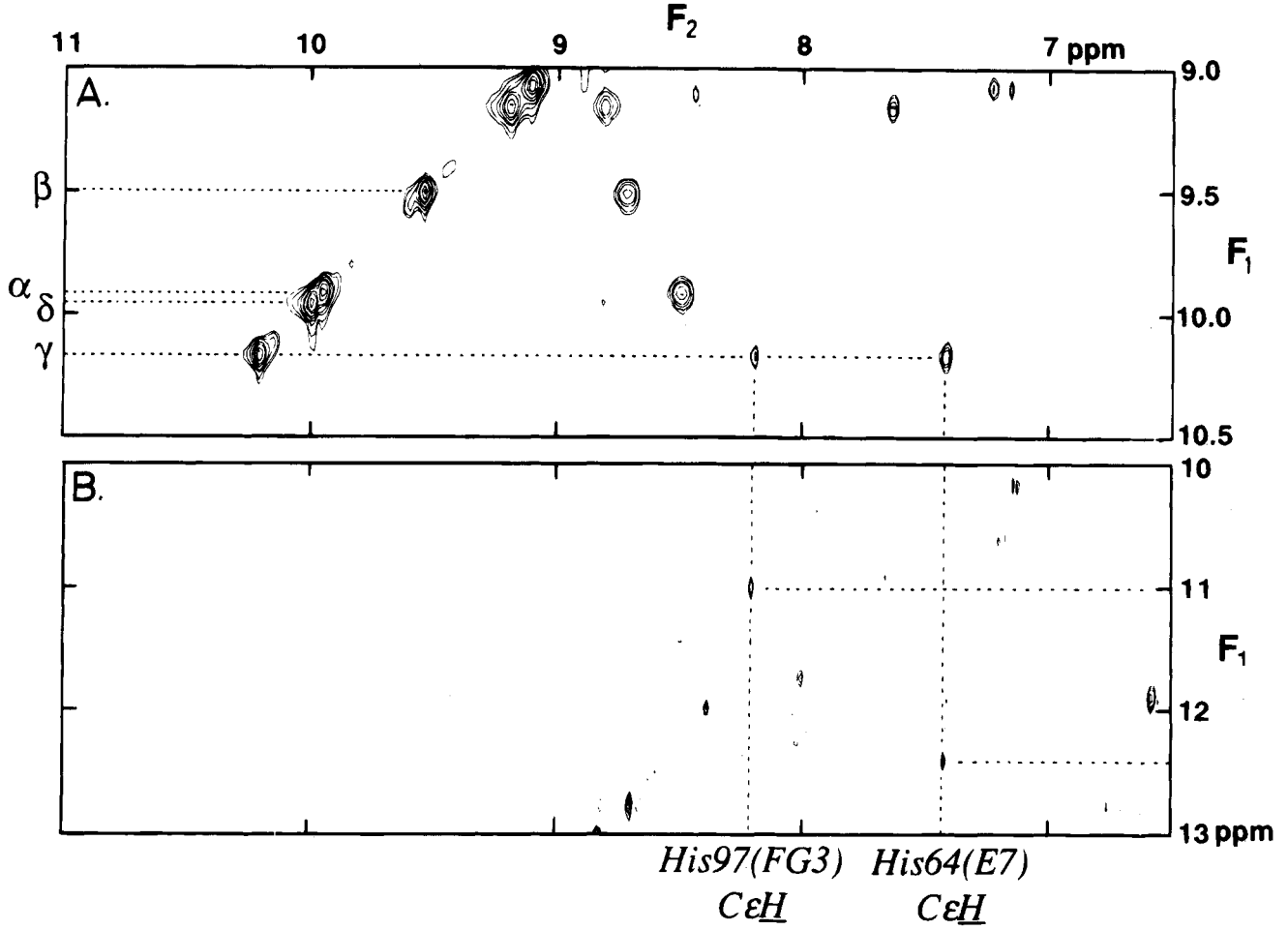

FIGURE 4: NOESY (A) and double quantum (B) spectra of the CO complex of Mb(S92A). α, β, δ, and γ show the signals from the porphyrin meso protons. The *γ-meso* proton signal affords cross peaks with His64(E7) imidazole $C^{\epsilon}H$ (7.42 ppm) and His93(FG3) imidazole $C^{\epsilon}H$ (8.20 ppm) in the NOESY spectrum. In the double quantum spectrum, the F1 value, which is the summation of the chemical shifts of His imidazole $C^{\epsilon}H$ and $C^{\delta}H$ signals, is 10.96 ppm for His93 or 12.40 ppm for His64.

(see Figures 2–5) are indicative of the structural change upon the mutation at 92(F8) position from Ser to Ala.

Distal Structure of Mb(S92A). In the spectral comparison, we note the NMR spectral feature of the CO complex of Mb(S92A) (see Table 2), where the proton signals of the distal residues such as Phe43(CD1), His64(E7), and Val68(E11) are essentially the same in their position as the corresponding ones of Mb(WT)CO. The resonance position of these proton NMR signals of Mb are predominantly determined by the porphyrin ring current, so that they are very sensitive to the configuration of these groups relative to the heme plane. Therefore, the observation of little change in their shifts is indicative of little structural change of these residues on the proximal mutation.

Support for this suggestion was provided from the IR spectrum of the CO complex of Mb(S92A), where we can observe the stretching mode of the iron-bound CO. The IR spectral feature, the absorption positions and the population of conformers, has been considered to be governed by the steric and/or electronic environment around the iron-bound CO which are encountered by the surrounding distal amino acid side chains. In the case of Mb(S92A)CO, the iron-bound CO stretching was observed and decomposed into three components at 1969, 1945, and 1932 cm^{-1} (data not shown), whose IR spectral feature was exactly the same as that of Mb(WT)CO (Adachi et al., 1992; Balasubramanian et al., 1993b).

So far, many mutants whose distal residues are substituted with other ones by site-directed mutagenesis have been reported. For the CO complexes of these mutants, it has been reported that the population of iron-bound CO conformers is different, and the methyl NMR signal of Val68 is changed in their shifts, compared with Mb(WT), due to structural changes at the distal side. Corresponding to these structural changes, the ligand binding kinetics are also drastically changed upon these mutations since the kinetic properties of Mb are substantially influenced by its distal structure. These are sharply contrasted to our present NMR and IR spectral data for Mb(S92A)CO. Furthermore, we observed that the association and the dissociation rate constants in the CO and the O_2 binding reactions were a little affected by the Ser92 mutation (see Table 3). Thus, we suggest that the mutation of Ser92 hardly influences the structure at the heme distal side of the CO complex of human Mb.

Little change in the distal structure of Mb upon replacing Ser92 with Ala was also confirmed in the cyanomet form, as demonstrated by the hyperfine-shifted NMR spectra (Table 4). In the spectral comparison, it was found that the signal of the distal His64(E7) imidazole $N^{\epsilon}H$ is unaltered in its position upon the mutation, while other signals are changed. For the distal His64 ring $N^{\epsilon}H$ in cyanomet hemoproteins, the hyperfine interaction is dipolar in origin, i.e., the through-space (pseudo-contact) interaction and depends on angular

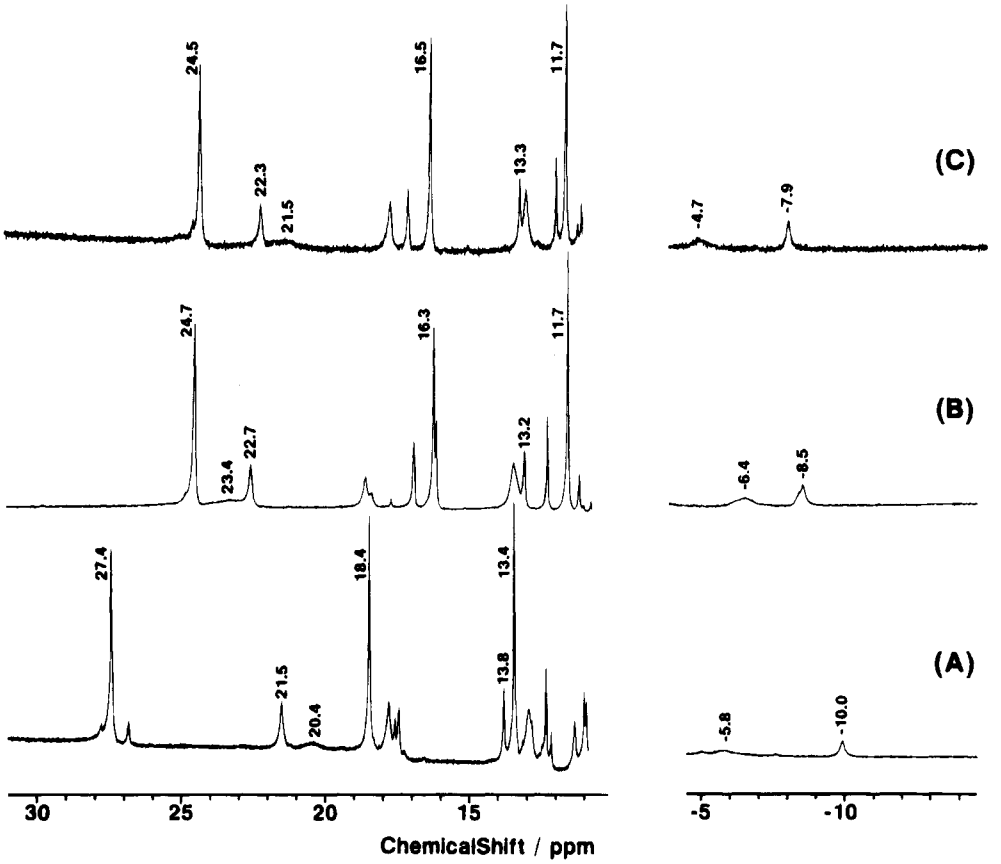

FIGURE 5: ^{1}H-NMR spectra of (A) Mb(WT), (B) Mb(S92A), and (C) Mb′(S92D) in the cyanomet form. The spectra were measured in 90% H_2O at 25 °C and pH 6.8. The signals around 23 ppm were not detected in 100% D_2O buffered solution. When we measured cyanomet Mb(S92A) in 90% H_2O at pH 8.0, the signal from the His64 N$^\epsilon$H was observed at 24 ppm as a shoulder peak of the 5-methyl signal.

Table 4: Assignment of ^{1}H-NMR Signals of the Cyanomet Form of Ser92 Mutant Myoglobins (ppm)

	Mb(S92A)	Mb′(S92D)	Mb(WT)
5-CH_3	24.7	24.5	27.4
1-CH_3	16.3	16.5	18.4
8-CH_3	11.7	11.7	13.4
His93 N$^\epsilon$H	22.7	22.3	21.5
His64 N$^\epsilon$H	24	24	24.5

variables as well as the inverse cube of the distance to the iron. No change in its chemical shift on the mutation implies that both the distance and the angular variables are exactly the same between the two proteins; no change in the distal structure in the cyanomet form between Mb(S92A) and Mb-(WT). Our suggestion concerning the distal structure of Mb-(S92A) is completely consistent with the X-ray crystal result by Smerdon et al. (1993).

On the other hand, we can see the difference in the hyperfine-shifted signals coming from the protons except for the distal His64 N$^\epsilon$H in the NMR spectra of the cyanomet form. This is also the case for the NOESY spectra of the CO form where the change in His97 C$^\epsilon$H and C$^\delta$H signals are detected. Now, we can interpret these spectral difference in terms of the structural difference at the heme proximal side between Mb(S92A) and Mb(WT). Further, we could extend this suggestion to the difference in the NMR and the resonance Raman spectra in the deoxy form (Figures 2 and 3).

Proximal Structure of the Ala92(F7) Mutant of Myoglobin. Since the His93 N$^\epsilon$H is a hydrogen-bonding partner of Ser92, the change of its ^{1}H-NMR signal position provides a piece of information about the electronic and structural character of the proximal imidazole. The hyperfine shift of the His93 N$^\epsilon$H signal in the deoxy form (Figure 2) has been shown to reflect overwhelmingly a contact interaction resulting from transfer of the iron electron spin into the imidazole σ system (La Mar & de Ropp, 1982). Thus, the downfield shift of this signal by 1.8 ppm upon the mutation corresponds to the increase in the spin density on this position transferred from the iron. If the hydrogen bond of His93 with Ser92 in Mb is strong enough to affect the electronic structure of its imidazole ring, the observed change of the His93 N$^\epsilon$H signal is reasonably consistent with the weakened or broken hydrogen bond upon the mutation. Alternatively, the NMR change can also be explained in terms of the compression of the Fe−N$^\delta$(His93) bond induced upon breaking the hydrogen bond of His93 N$^\epsilon$H by replacing Ser92 to Ala. Hereby, we noted that the Fe−N$^\delta$(His93) Raman stretching band showed a high frequency shift by 3 cm^{-1} upon the mutation from Ser92 to Ala. According to the suggestion by La Mar et al. (1982), the NMR and the Raman spectral changes on the present mutation are probably consistent with the structural change around the Fe−His93 bond rather than the electronic change in the His93 imidazole ring.

One of the possible changes in the proximal structure of Mb on the mutation from Ser92 to Ala can be suggested from the NMR measurements of the cyanomet forms (see Figure 5). It is generally accepted that the hyperfine shifts of the heme methyl proton NMR signals for cyanomet hemoproteins are mainly governed by the interaction of the p_π-orbital of the N$^\delta$ of His93 with the iron d_z orbitals where the unpaired electron resides. On the basis of this idea,

Yamamoto et al. (1990) recently reported a simple correlation of the chemical shift (δ) of the heme methyl proton signals of the cyanomet hemoproteins with the angle (Φ) between the projection of the proximal imidazole plane onto the heme plane and the porphyrin N_2-N_4 vector [see Figure 3 in Yamamoto et al. (1990)]. The chemical shifts of the heme methyl for Mb(S92A)$^+$CN$^-$ fall in their plots δ vs Φ between those of sperm whale Mb ($\Phi = 19°$) and *Aplysia limacina* Mb ($\Phi = 29°$). Thus, the mutation of Ser92 to Ala makes the imidazole plane rotate clockwise by about 5° from the native position around the Fe−His93 bond, with the heme viewed from the distal side. This result is quite different from the X-ray structure of the Ser92 mutation of pig Mb reported by Smerdon et al. (1993), where no rotation of the His93 imidazole around the Fe−N$^\delta$(His93) was observed. It is possible that the change is too small to be discerned at 2.7-Å resolution reported by these authors.

In the crystal data of pig Mb(S92L) in the aquomet state (Smerdon et al., 1993), the most remarkable change on the Ser92 mutation is the rotation of the His97 imidazole ring away from the C-terminus of the F-helix around the $C^\alpha-C^\beta$ bond. However, in the NMR spectrum of human Mb(S92A)-CO, the NOE cross peak was detectable between the His97 imidazole C$^\epsilon$H and the porphyrin *γ-meso* proton (see Figure 4), indicating that the distance between these two protons is not drastically changed in the solution state upon this mutation. On the other hand, we also found in the NMR spectrum of Mb(S92A)CO that the change of the His97 signal position is relatively larger than those of any other signals (see Table 3). The His97 imidazole ring is parallel and close to the heme plane on the heme proximal side, so that the resonance positions of its C$^\epsilon$H and C$^\delta$H NMR signals are predominantly influenced by the porphyrin ring current. Therefore, the change of the His97 imidazole signals is indicative of the change of the relative position of the imidazole plane to the porphyrin plane. Comparing the C$^\epsilon$H and the C$^\delta$H signal positions among Mb(S92A) and Mb(WT), the Ser92 mutation causes the C$^\epsilon$H signal to shift upfield, while the C$^\epsilon$H shifts downfield (Table 3). This change can be consistently explained in terms of the flip of the imidazole plane around the His $C^\beta-C^\gamma$ bond; the C$^\epsilon$H goes away from but the C$^\delta$H comes near the heme plane.

As a consequence, the structural change at the His97 imidazole upon the Ser92 mutation was also detectable in the solution state of Mb, but the change is not so drastic as that found in the crystal structure. This discrepancy may reflect either the difference between the crystal and the solution structure of Mb. From this comparison, it is likely to suggest that some substates exit in the proximal structure of the Ser92 mutant of Mb. The solution structure evaluated by the spectroscopic methods is the average of them, and one of them is probably responsible for the easy heme dissociation and the second isocyanide binding to the iron at the proximal side, which were reported by Smerdon et al. (1993).

Asp92(F7) Mutant of Myoglobin. We attempted to prepare Mb(S92D) as a model of the strong hydrogen-bonded N$^\epsilon$H of the proximal His93 (Poulos et al., 1980). However, Mb′(S92D) is expressed in *E. coli* in very low level. This is likely because the protein is digested by some proteases in *E. coli* as the purified Mb′(S92D) is also unstable to tryptic digestion. Surprisingly the NMR spectral features of Mb′(S92D) in the deoxy (Figure 2) and cyanomet (Figure 5) forms closely resemble the corresponding features of Mb(S92A), suggesting that there is no hydrogen bond interaction of His93 N$^\epsilon$H in Mb′(S92D). In the Ser residue, the hydrogen bonding point is at the second atom from the main chain, but at the third atom in Asp. Possibly, the geometry of the hydrogen bond with the His93 imidazole N$^\epsilon$H in Mb is so strict that it would not be allowed for the Asp92 carboxylate.

ACKNOWLEDGMENT

We thank Mr. Motoyasu Fujii for his work in the kinetic measurements of the CO and O_2 binding reaction.

REFERENCES

Adachi, S., Nagano, S., Watanabe, Y., Ishimori, K., & Morishima, I. (1991) *Biochem. Biophys. Res. Commun. 180*, 138−144.

Adachi, S., Sunohara, N., Ishimori, K., & Morishima, I. (1992) *J. Biol. Chem. 267*, 12614−12621.

Adachi, S., Nagano, S., Ishimori, K., Watanabe, Y., Morishima, I., Egawa, T., Kitagawa, T., & Makino, R. (1993) *Biochemistry 32*, 241−252.

Balasubramanian, S., Lambright, D. G., & Boxer, S. G. (1993a) *Proc. Natl. Acad. Sci. U.S.A. 90*, 4718−4722.

Balasubramanian, S., Lambright, D. G., Marden, M. C., & Boxer, S. G. (1993b) *Biochemistry 32*, 2202−2212.

Cheng, X., & Schoenborn, B. P. (1991) *J. Mol. Biol. 220*, 381−399.

Dalvit, C., & Wright, P. E. (1987) *J. Mol. Biol. 194*, 313−327.

Emerson, S. D., & La Mar, G. N. (1990) *Biochemistry 29*, 1556−1566.

Evans, S. V., & Brayer, G. D. (1990) *J. Mol. Biol. 213*, 885−897.

Higgins, D. G., & Sharp, P. M. (1988) *Gene 73*, 237−244.

La Mar, G. N., & de Ropp, J. S. (1982) *J. Am. Chem. Soc. 104*, 5203−5206.

La Mar, G. N., Budd, D. L., & Goff, H. (1977) *Biochem. Biophys. Res. Commun. 77*, 104−110.

Lambright, D. G., Balasubramanian, S., & Boxer, S. G. (1989) *J. Mol. Biol. 207*, 289−299.

Oldfield, T. J., Smerdon, S. J., Dauter, Z., Petratos, K., Wilson, K. S., & Wilkinson, A. J. (1992) *Biochemistry 105*, 1522−1527.

Perutz, M. F. (1970) *Nature (London) 228*, 726−739.

Poulos, T. L., Freer, S. T., Alden, R. A., Edwards, S. L., Skogland, U., Takio, K., Eriksson, B., Xuong, N.-U., Yonetani, T., & Kraut, J. (1980) *J. Biol. Chem. 255*, 575−580.

Quillin, M. L., Arduini, R. M., Olson, J. S., & Phillips, G. N., Jr. (1993) *J. Mol. Biol. 234*, 140−155.

Sato, T., Tanaka, N., Neya, S., Funasaki, N., Iizuka, T., & Shiro, Y. (1992) *Biochem. Biophys. Acta 1121*, 1−7.

Smerdon, S. J., Krzywda, S., Wilkinson, A. J., Brantley, R. E., Jr., Carver, T. E., Hargrove, N. S., & Olson, J. S. (1993) *Biochemistry 32*, 5132−5138.

Varadarajan, R., Lambright, D. G., & Boxer, S. G. (1989) *Biochemistry 28*, 3771−3781.

Yamamoto, Y., Nanai, N., Chujo, R., & Suzuki, T. (1990) *FEBS Lett. 264*, 113−116.